All Sciences Proceedings

1st International Conference on Recent and Innovative Results in Engineering and Technology

August 16-18, 2023 : Konya, Turkey

ICRIRET

All Sciences Proceedings
http://as-proceeding.com/

https://as-proceeding.com/index.php/icriret

A one-dimensional modeling tool for solar cells called SCAPS on CZTS/ZnS

Serap YIGIT GEZGIN[1], Silan BATURAY[2], Hamdi Sukur KILIC[1,3,4]

[1]*Department of Physics, Faculty of Science, University of Selcuk, 42031 Selcuklu, Konya, Turkey*

[2]*Department of Physics, Faculty of Science, Dicle University, 21280 Diyarbakir, Turkey*

[3]*Directorate of High Technology Research and Application Center, University of Selcuk, 42031 Selcuklu, Konya, Turkey*

[4]*Directorate of Laser Induced Proton Therapy Application and Research Center, University of Selçuk, 42031 Konya, Turkey*

**Corresponding author e-mail: silan@dicle.edu.tr*

Abstract – In the study, Zinc sulphide thin films were deposited related to different annealing ambient by ultrasonic spray pyrolysis technique (USP) on soda lime glass substrates. Optical properties of these films were analyzed by using ultraviolet–visible (UV–Vis) spectrophotometry at room temperature. Ultraviolet–visible spectroscopy measurements indicate that all ZnS thin films indicated high extinction coefficient in the NIR region. ZnS thin films, which was un annealed and annealed at N_2 atmosphere show higher skin depth in the low and high energy bands. However, the skin depth of ZnS thin film annealed at 500 ^{O}C at H_2S:Ar (1:10) is the lowest compared to the other thin films. Au/CZTS/ZnS-500&ZnS-550/i-ZnO/AZO solar cells that is modelled by SCAPS simulation. The increase of the shallow donor defect density (N_D) and Auger electron/hole capture coefficient that deteriorated photovoltaic performance. After Auger electron/hole capture coefficient=10^{-24} cm^6/s, there are recombined that more electrons from the charge carriers formed in ZnS thin film annealed at 500 ^{O}C at H_2S:Ar. SnO_2 intermediate layer, is placed between CZTS and ZnS layers, caused more charge separation at the two interfaces and increased V_{oc} and efficiency of the solar cell.

Keywords – ZnS Thin Film, Skin Depth, Auger Electron/Hole Capture, SCAPS Simulation

1. Introduction

Zinc sulphide (ZnS) is an important II-VI semiconducting material having a large direct band gap in the bulk of 3.65 eV [1]. It could be used in optoelectronic devices like blue light emitting diodes [2], devices of electroluminescent and photovoltaic cells [3]. A CdS buffer layer is often necessary to achieve high conversion efficiency in thin film solar cells based on $CuGaIn(S,Se)_2$ absorbers. Regarding the creation and application of the CdS layer, there are hazardous risks. Therefore, it has been suggested to conduct research on creating Cd-free buffer layers. This prompted researchers to look at using the zinc sulphide as a buffer layer in Glass/Mo/$CuInS_2$/buffer/ZnO devices. [4]. Compared to CdS, ZnS has a broader energy band, which allows for additional high-energy photons being transferred to the junction and an improvement in the solar cells' blue response. a number of methods, including thermal evaporation [5], ultrasonic radiation [6], triple codoping [7], hydrothermal [8], chemical bath deposition [9], and ultrasonic spray pyrolysic [10]. The basis of the ultrasonic spray pyrolysis process is the source solution's thermal breakdown after being sprayed by an nozzle onto the thermally heated surface of substrate. Simply adding an element to the aqueous solution allows for the large-scale fabrication of films with almost any ingredient in any proportion [11]. Additionally, spray pyrolysis may be

accomplished without vacuum and does not require high-quality targets. By adjusting the spray settings, it is simple to manage the layer thickness and deposition rate. The spray pyrolysis method is used in this study to produce ZnS thin films on the SLG substrates due to its ease of use and adaptability.

In this study, we primarily used the well acclaimed simulation tool SCAPS (Solar Cell Capacitance Simulator), a windows-oriented application created at the University of Gent using LabWindows/CVI from National Instruments. A one-dimensional modeling tool for solar cells called SCAPS was attained for the CIGS, $CuInSe_2$, and CdTe families of cells[12]. However, this program has undergone a number of changes that enhance its capacity to operate with both crystalline solar cells and amorphous cells [13]. For thin film polycrystalline solar cells, the necessity for numerical modeling is pertinent due to the complexity of the absorber/buffer interface including hetero-junctions [14, 15]. The most AC and DC electrical measures that can be computed in both low- and high-light conditions, as well as at various temperatures, are found in SCAPS. These measurements include the open circuit voltage (*Voc*), short circuit current density (*Jsc*), fill factor (*FF*%), and others.

Particular effort has been focused on enhancing Cd-free absorber layers in solar cells. As a result, ZnS films have received far more attention in recent years than their bulk counterparts. In this work, ZnS films were produced at 350°C using the USP process. The ZnS films were then annealed in an H_2S, air and N_2 environment, to develop their characteristics. The annealed effect at different temperatures (500 ^{O}C and 550 ^{O}C) was thoroughly explored, however the optical and photovoltaic characteristics of the films in different annealing temperatures in H_2S:Ar(1:10) environment were not thoroughly investigated using the SCAPS software. As a result, we present the structural and optical characteristics of ZnS films made by USP under various annealing environments. The influence of operating temperature, density of electron, and defect on the zinc sulphide (ZnS) buffer layer and cell performance is investigated here, and ZnS is used as the buffer layer and CZTS as the absorber layer. In the SCAPS 3302 environment, a CZTS thin-film solar cell made of SLG/Mo/CZTS/buffer layer/Al:ZnO was constructed. Both the operating temperature and the light spectrum were set by default to 300 K and the global AM1.5 standards.

1. Experimental

Using the ultrasonic spray pyrolysis (USP) process in an environment of N_2 to eliminate oxidation, ZnS thin films were initially produced for deposition on soda lime glass (SLG) substrate. Various steps were used for SLG substrate cleaning process: firstly, substrates were boiled in a mixture of 5:1:1 distilled water, ammonia, and hydrogen peroxide for 20 min at 95 °C, secondly, in 5:1:1 distilled water, hydrogen peroxide, and hydrocholoric acid for 20 min at 95 °C. Then, ultrasonicated in ethanol~5 min and after then, the substrates were cleaned in deionized water for 5 minutes before being dried in N_2 gas to eliminate any remaining distilled water from their surface. To make ZnS thin films, a stoichiometric quantity of 0.1 M zinc acetate ($Zn(CH_3COO)_2$), 0.2 M thiourea ($SC(NH_2)_2$ in deionized water was utilized. Thiourea is very volatile nature at high temperatures [16]. As a result, this component was added twice to avoid sulphur loss Separately manufactured, the chemical with a 1:1 stoichiometric ratio was combined for two hours at room temperature on a magnetic stirrer with 30 ml deionized water and a trace quantity of diethanolamine to control the pH level. The obtained ZnS solution was atomized using ultrasonic nebulizer (SonoTek Exacta-Coat) onto SLG with a frequency of 125 kHz. On the SLG heated to about 350 °C with a constantly fixed nozzle-substrate spacing of 9.5 cm, the resulting solution was sprayed using USP. During the spraying operation, the nozzle was continually run at 125 kHz, producing drops with a median diameter of 8 lm. During a 50-minute period, 60 cc of the produced solution was sprayed onto the substrates. The ZnS solution flow rate was kept around 1 mL/min and controlled via flow meter, transported by N_2 gas to the substrate to eliminate the formation of oxidation. ZnS thin films were annealed at 500 °C in air, 500 °C in N_2, H_2S:Ar (1:10) at 500 °C and H_2S:Ar (1:10) at 550 °C for 60 min in a quartz furnace, respectively to study the annealed effect. The skin depth and extinction coefficient of the ZnS thin films was calculated in UV-Vis spectrophotometer in the wavelength range of 300–1100 nm under air atmosphere. Now in our study,

we will use zinc sulfide (ZnS) as absorber layer and cadmium sulfide (CdS) as buffer layer. The key theme of this model is to understand the possibility of the material for absorber layer on CdS for buffer layer. ZnS thin-film solar cell with the structure of Mo/*p*-CZTS/ZnS-500&ZnS-550/I-ZnO/AZO was implemented in the SCAPS 1-D simulation program. The default lighting scale and operation temperature were fixed to the global AM1.5 standards and 300 K, respectively.

2. Discussion

2.1. The optical feature of ZnS thin films

The electric field formed between the carrier charges in the thin film, which represents the dielectric coefficient that is a parameter that defines the charge mobility in the thin film and affects the charge accumulation in the thin film solar cell. In this context, the static dielectric constant (ε_o) and high frequency dielectric constant (ε_∞) values are designed with Eq (1) and Eq (2), respectively:

$$\varepsilon_o = 18.52 - 3.08E_g \quad (1)$$

$$\varepsilon_\infty = n^2 \quad (2)$$

Since all ZnS samples have wide band gaps, their refractive indices and dielectric coefficients are somewhat low. Furthermore, ZnS-As grown thin film presents the lowest dielectric constants. In this thin film, the charge carriers' lifetime and charge transitions may be limited, the charge mobility may become unstable [17, 18]. The results obtained with Moss and Herve&Vandemme relations are not very different from each other.

Table 1. Refractive index (n), high frequency dielectric constant (ε_∞) and static dielectric constant (ε_o) of ZnS thin films with ambients of as grown, air, N_2, H_2S at 500 ^{O}C and H_2S at 550 ^{O}C

Samples	E_g (eV)	Moss relation		Herve&Vandemme		Static Dielectric Constant, ε_o
		n	ε_∞	n	ε_∞	
ZnS-As grown	3.75	2.31	5.36	2.14	4.61	6.87
ZnS-Air	3.58	2.34	5.49	2.19	4.79	7.49
ZnS-N2	3.66	2.33	5.43	2.17	4.71	7.24
ZnS-500	3.68	2.32	5.41	2.16	4.68	7.18
ZnS-550	3.70	2.32	5.40	2.16	4.67	7.12

In the thin film, light loss by scattering and absorption can occur and is denoted by the extinction coefficient (k) [19]:

$$k = \frac{\alpha\lambda}{4\pi} \quad (3)$$

λ; wavelength of the incident light. The absorption coefficient (α) of thin films can be calculated via $\alpha = 2.303 \times (\frac{A}{T})$ equation. A and T, which are the absorbance and thin film thickness, respectively. Since the ZnS-550 thin film has high absorption, its extinction coefficient is higher compared to other samples. In the NIR region, all ZnS thin films indicated high extinction coefficient.

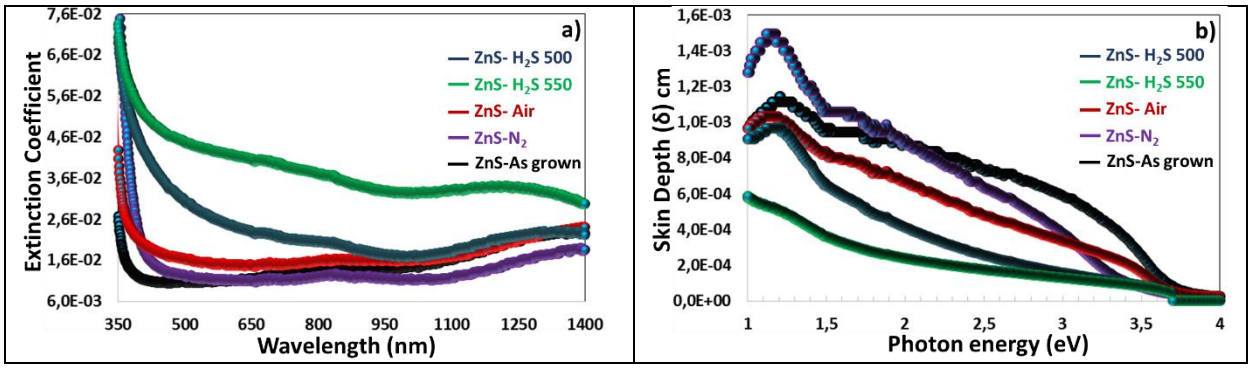

Figure 1. a) The extinction Coefficient and b) the skin depth of ZnS thin films with ambients of as grown, air, N_2, H_2S at 500 ^oC and H_2S at 550 ^oC

The light incident on the thin film travels through the film depending on the wavelength and the extinction coefficient. This path taken by the light is defined as the skin depth (χ) expressed by Eq. (4) [19]:

$$\chi = \frac{\lambda}{2\pi k} \quad (4)$$

ZnS-N_2 and ZnS-As grown thin films which show higher skin depth in the low and high energy bands, respectively. However, the skin depth of ZnS-550 thin film is the lowest compared to the other thin films. Since the ZnS-550 thin film has the highest grain size, its photon absorption is higher and the light transmission is low. Thus, the skin depth is reduced. This optical property is not very suitable for use as a buffer layer in solar cells, although it has the most advance crystal structure. However, ZnS-500 thin film has a slightly lower crystalline structure than ZnS-550 and has a higher skin depth.

3. *Determination of photovoltaic parameters of ZnS thin films*

3.1. *The effect of Auger electron/hole capture coefficient on PV performance of ZnS-500/CZTS solar cell*

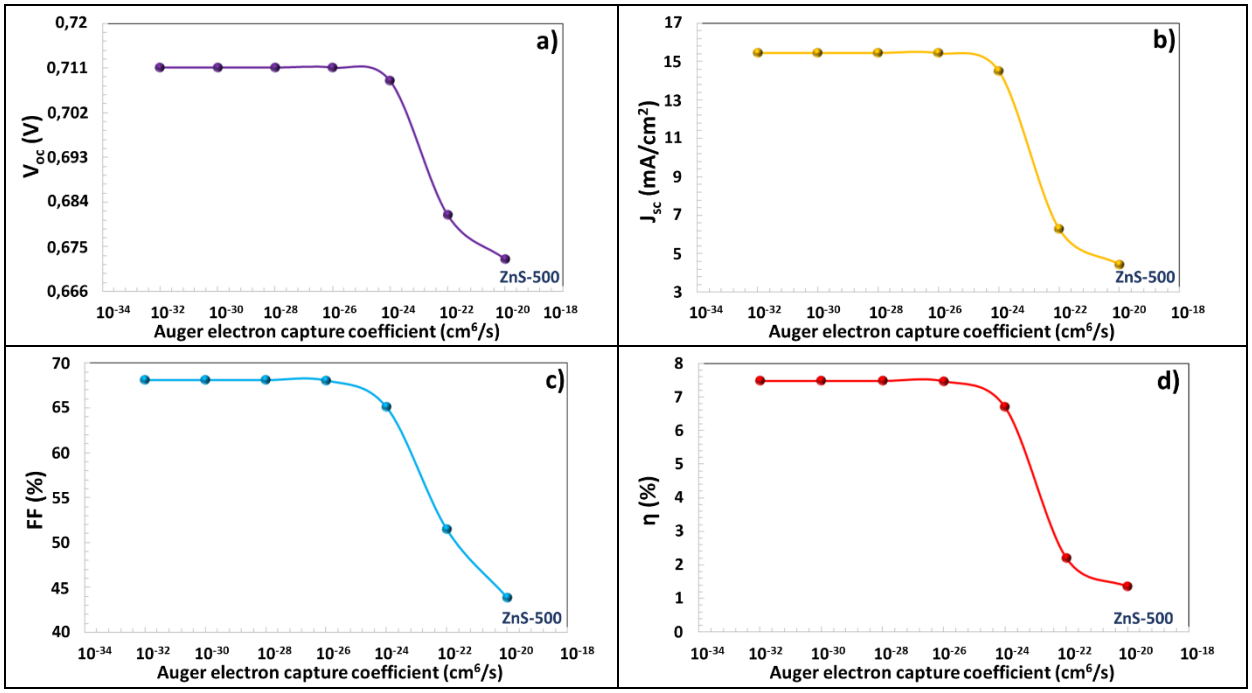

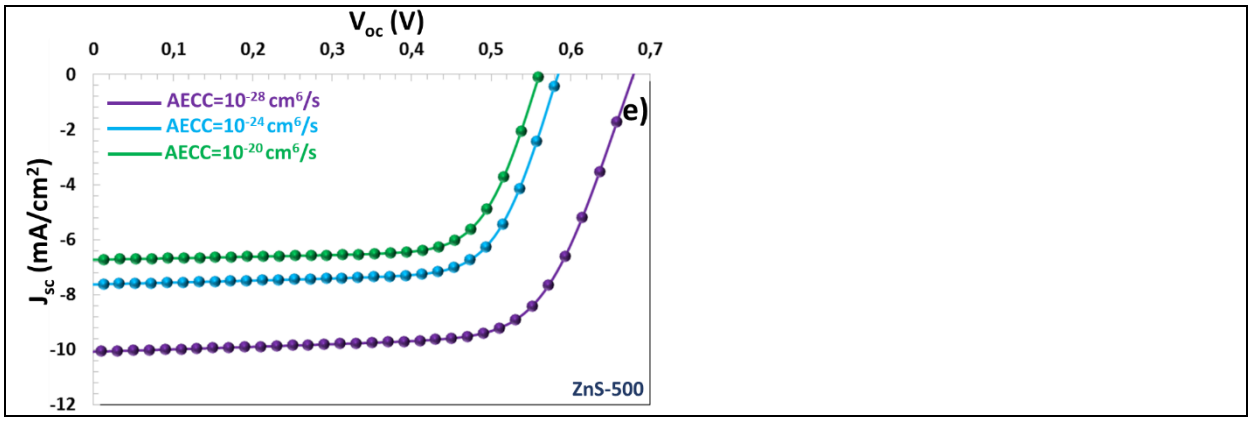

Figure 2. (a-d)The characteristics of the photovoltaic parameters vs Auger electron capture coefficient, e) $J-V$ characteristic for ZnS-500/CZTS solar cell

Table 2. The photovoltaic parameters of CZTS/ZnS-500 heterojunction solar cell

Auger electron capture coefficient (cm^6/s)	V_{oc} **(V)**	J_{sc} **(mA/cm^2)**	FF **(%)**	η **(%)**
10^{-32}	0.711	15.44	68.11	7.48
10^{-30}	0.711	15.44	68.11	7.48
10^{-28}	0.711	15.44	68.11	7.48
10^{-26}	0.711	15.43	68.07	7.47
10^{-24}	0.708	14.52	65.10	6.70
10^{-22}	0.681	6.29	51.48	2.21
10^{-20}	0.672	4.44	43.88	1.35

As a consequence of the recombination of electrons and holes, an excess of energy is released. But instead of emitting photons with this energy, the electrons are excited to higher energy levels in the conduction or valence band. This process is known as the Auger recombination. Auger electron or hole recombination, which takes place without radiation, negatively affects the photovoltaic behaviour of the solar cell [20, 21]. The characteristics of the photovoltaic parameters of ZnS-500/CZTS solar cell that calculated based on the Auger electron capture coefficient (AECC) are given in the Figure 2. There was no change in the photovoltaic parameters for the AECC value between10^{-32} cm^6/s and 10^{-26} cm^6/s ranges. As the AECC value increased from 10^{-26} cm^6/s to 10^{-20} cm^6/s, the V_{oc}, J_{sc}, FF and η values decreased from 0.711 V to 0.672 V, from 15.43 mA/cm^2 to 4.44 mA/cm^2, from 68.07% to 43.88%, from 7.48 % to 1.35%, respectively. Furthermore, in the study based on the Auger hole capture coefficient (AHCC), when AHCC is increased from 10^{-32} cm^6/s to 10^{-26} cm^6/s, there is no change in the performance of the ZnS-500/CZTS solar cell. When it is increased from 10^{-26} cm^6/s to 10^{-22} cm^6/s, V_{oc}, J_{sc}, FF and η, which diminished from 0.711 V to 0.680 V, from 15.00 $mAcm^{-2}$ to 9.70 $mAcm^{-2}$, from 68.11 % to 60.56 %, from 7.48 % to 3.99 %, respectively. The performance of the solar cell deteriorated after AHCC and AECC values in 10^{-26} cm^6/s in the *n*-type ZnS semiconductor. Since Auger electron/hole recombination is a non-radiative recombination process, it showed a similar effect in ZnS with major electron charge carriers.

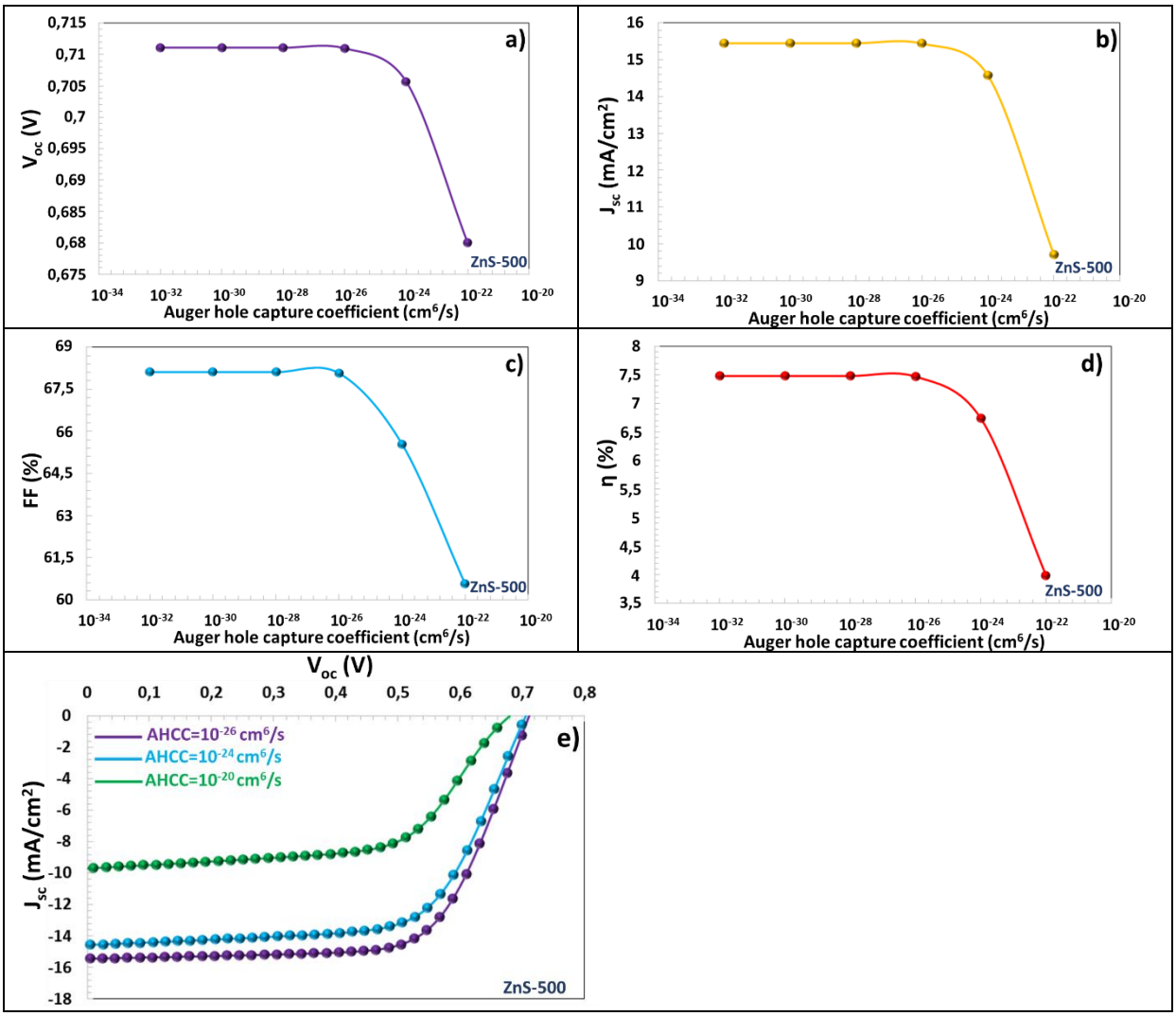

Figure 4. (a-d)The characteristics of the photovoltaic parameters vs Auger hole capture coefficient, e) $J-V$ characteristic for ZnS-500/CZTS solar cell

Table 3. The photovoltaic parameters of CZTS/ZnS-500 heterojunction solar cell on Auger hole capture coefficient

Auger hole capture coefficient (cm^6/s)	V_{oc} **(V)**	J_{sc} **(mA/cm^2)**	FF **(%)**	η **(%)**
10^{-32}	0,7111	15	68,11	7,48
10^{-30}	0,7111	15,4492	68,11	7,48
10^{-28}	0,7111	15,449	68,11	7,48
10^{-26}	0,711	15,4381	68,07	7,47
10^{-24}	0,7057	14,5686	65,54	6,74
10^{-22}	0,68	9,7006	60,56	3,99

3.2. The effect of the generation/recombination on PV performance of ZnS-500/CZTS solar cell

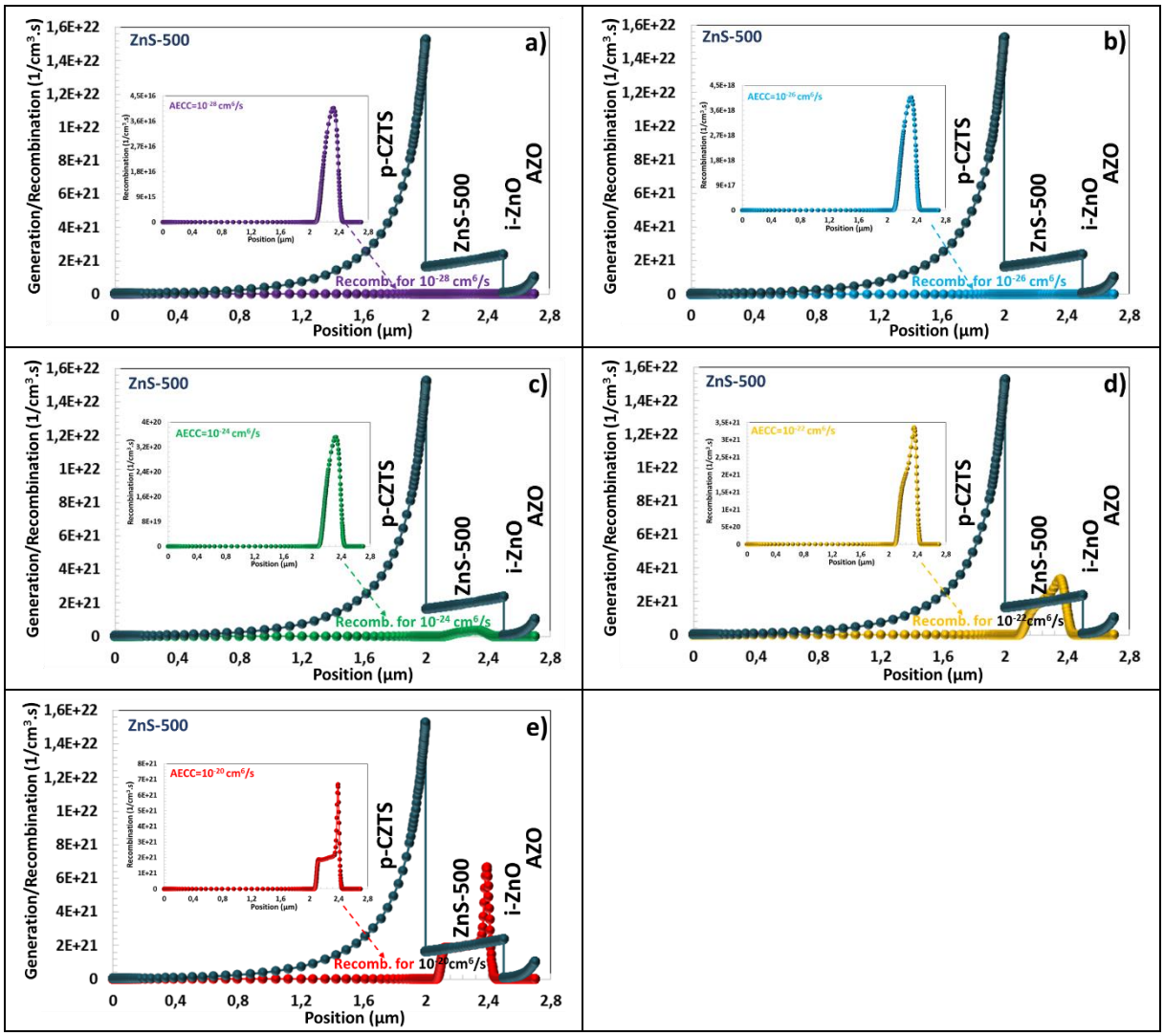

Figure 5 The characteristic of the generation/recombination (electron) vs position in band diagram of CZTS/ZnS-500 heterojunction solar cell

The photo excited electron-hole pair is formed by excitation of the electron in the valence band by the photon incident on a semiconductor thin film. The group of electron or hole charge carriers develops the *n*-type or *p*-type conductivity of semiconductors. In the generation characteristic in the Figure 5 more photo-excited charge carriers are shaped in the thick CZTS absorber layer[22, 23] . In the ZnS thin film in 500 nm thickness, charge carriers in 1.65×10^{21} $1/cm^3.s$ and 2.37×10^{21} $1/cm^3.s$, which are formed at position = 2.001 µm and = 2.5 µm, respectively. Fewer charge carriers were formed in ZnS semiconductor at the boundary of the depilation region. In this case, photo-excited charge carriers are reduced as some of the incident light on ZnS that is absorbed in this thin film. Conversely, when light first comes to the ZnS surface, it forms more photo excited charge carriers without being absorbed too much. For AECC=10^{-28} cm^6/s, the electrons in 3.94×10^{16} $1/cm^3.s$ that are captured at position= 2.345 µm in ZnS thin film. The electrons in 6.50×10^{21} $1/cm^3.s$ that are recombined at position=2.395 µm for AECC=10^{-20} cm^6/s. With the increase of AECC, more electron charge carriers were subjected to recombination in the thin film. After AECC=10^{-24} cm^6/s, there are recombined that more electrons from the charge carriers formed in ZnS thin film. As can be seen in the Figure 5, the efficiency of the solar cell decreased significantly for AECC=10^{-22} cm^6/s and 10^{-20} cm^6/s values.

3.3. The effect of SnO2 intermediate layer on PV performance of ZnS-500/CZTS solar cell

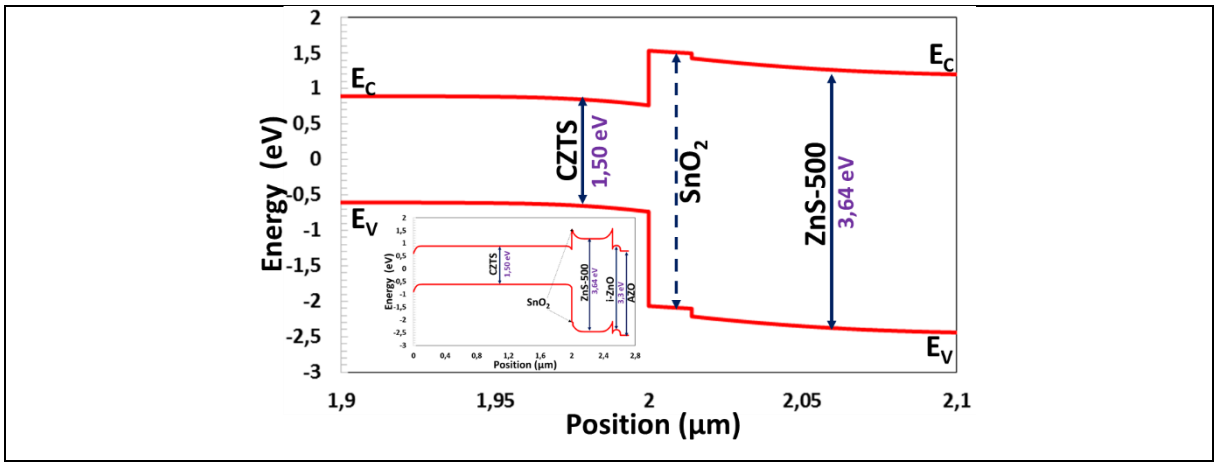

Figure 6. The band gap diagram of CZTS/SnO_2/ZnS-500 solar cell

The irregular band alignment, the pin holes, cracks, hanging bonds, and leakage paths occur at the interface of the solar cell, resulting in recombination of charge carriers within traps and defects, the parasitic paths which cause deterioration in the performance of the solar cell. Adding SnO_2 intermediate layer to the heterojunction interface is one of the most effective ways to passivate these interfacial states. The SnO_2 intermediate layer limits recombination by passivating the interfacial states between the CZTS and ZnS semiconductors [24, 25]. In addition, it optimizes the band alignment of the valance and conduction of the semiconductors. Furthermore, the very thin SnO_2 layer leads to more charge separation at the interface and charge accumulation at the boundaries of the depletion region. Thus, there is a significant enhance in the voltage and power exchange efficiency of the solar cell. The transition of electrons in the conduction band of CZTS to the conduction band of ZnS becomes easier.

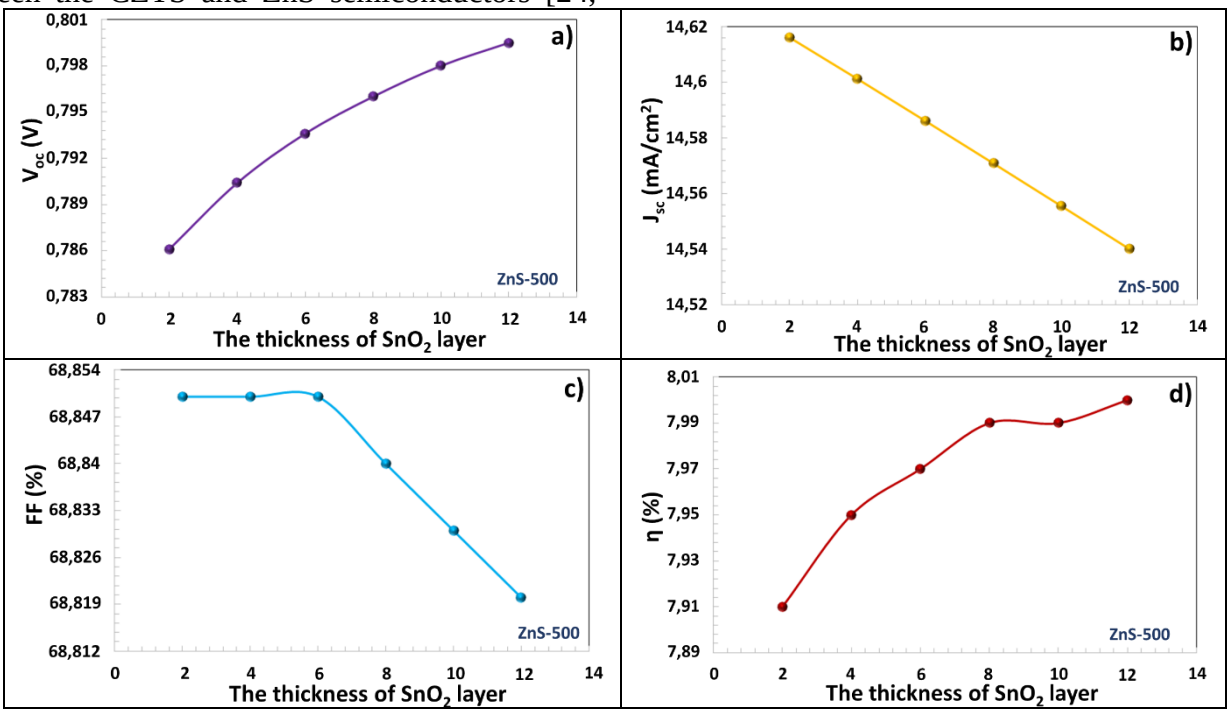

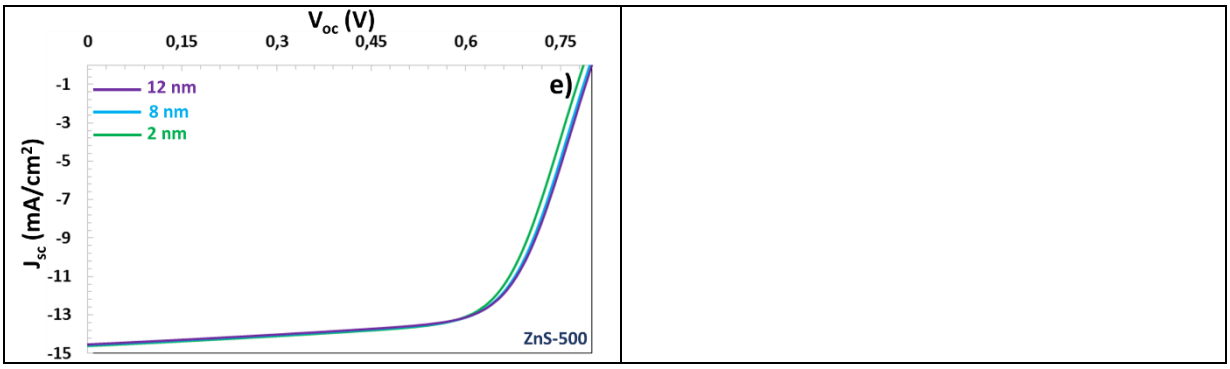

Figure 7. (a-d) The variation characteristics of the photovoltaic parameters and e) $J-V$ curve of CZTS/SnO_2/ZnS solar cell depending on the thickness of SnO_2 intermediate layer

The thickness of the SnO_2 layer can change the efficiency of the solar cell [26]. According to the variation characteristic of the photovoltaic parameters depending on the SnO_2 film thickness in the Figure 7, as the thickness of the SnO_2 layer increased, V_{OC} and efficiency increased, while J_{sc} and FF decreased. In very thin thickness, sufficient charge separation does not occur. However, increasing film thickness caused an increase in the electrical field in the depletion region. The electric field leads to that the positive and negative charges to increase further. As the electric field increases, the established voltage value in the depletion region increases. As a result, the voltage of the solar cell rises. However, As the film thickness increases, the number of photons reaching the CZTS layer decreases that causes the photocurrent and J_{sc} value to decrease.

CONCLUSIONS:

UV-Vis spectrophotometry was used to characterize the optical characteristics of these films. Ultraviolet-visible spectroscopy experiments show that all ZnS thin films have a high extinction coefficient in the near-infrared range. Thin films with increased skin depth have been produced using ZnS-N_2 and ZnS-As-grown. The solar cell consisting of Au/CZTS/ZnS-500&ZnS-550/i-ZnO/AZO layers was modelled with the SCAPS-1D program. The increase on N_D in ZnS thin films causes doping and reduction of the electric field in the depilation region, thus deteriorating the photovoltaic performance. With the increase of Auger electron/electron capture coefficient, electrons are excited to high energy level by non-radiative path and Auger recombination of charge carriers occurs and all PV parameters of the solar cell are decreased. After AECC=10^{-24} cm^6/s, there are recombined that more electrons from the charge carriers formed in ZnS thin film. The SnO_2 intermediate layer limits recombination by passivating the interfacial states between the CZTS and ZnS semiconductors. Thus, there is a significant enhance in the voltage and power conversion efficiency of the solar cell.

Acknowledgements

Authors would kindly like to thank to

- Selcuk University, Scientific Research Projects (BAP) Coordination Office for the support with the number 15201070 and 19401140 projects,
- Selçuk University, High Technology Research and Application Center (İL-TEK) and
- SULTAN Center for infrastructures

Dr. Marc Burgelman's group, University of Gent, Belgium for providing permission for us to use SCAPS-1D simulation program

Reference

1. Gao, X., X. Li, and W. Yu, *Morphology and optical properties of amorphous ZnS films deposited by ultrasonic-assisted successive ionic layer adsorption and reaction method.* Thin solid films, 2004. **468**(1-2): p. 43-47.
2. Nasr, T.B., et al., *Effect of pH on the properties of ZnS thin films grown by chemical bath deposition.* Thin solid films, 2006. **500**(1-2): p. 4-8.
3. Vidal, J., et al., *Influence of magnetic field and type of substrate on the growth of ZnS films by chemical bath.* Thin Solid Films, 2002. **419**(1-2): p. 118-123.
4. Calderón, C., et al., *Studies in CuInS2 based solar cells, including ZnS and In2S3 buffer layers.* Materials science in semiconductor processing, 2013. **16**(6): p. 1382-1387.

5. Li, Q. and C. Wang, *Fabrication of wurtzite ZnS nanobelts via simple thermal evaporation.* Applied physics letters, 2003. **83**(2): p. 359-361.
6. Xu, J., et al., *Preparation of ZnS nanoparticles by ultrasonic radiation method.* Applied Physics A, 1998. **66**: p. 639-641.
7. Yamamoto, T., S. Kishimoto, and S. Iida, *Control of valence states for ZnS by triple-codoping method.* Physica B: Condensed Matter, 2001. **308**: p. 916-919.
8. Hoa, T.T.Q., T.D. Canh, and N.N. Long. *Preparation of ZnS nanoparticles by hydrothermal method*. in *Journal of Physics: Conference Series*. 2009. IOP Publishing.
9. Long, F., et al., *An improved method for chemical bath deposition of ZnS thin films.* Chemical Physics Letters, 2008. **462**(1-3): p. 84-87.
10. Bang, J.H., R.J. Helmich, and K.S. Suslick, *Nanostructured ZnS: Ni2+ photocatalysts prepared by ultrasonic spray pyrolysis.* Advanced Materials, 2008. **20**(13): p. 2599-2603.
11. Bang, J.H., et al., *Porous carbon supports prepared by ultrasonic spray pyrolysis for direct methanol fuel cell electrodes.* The Journal of Physical Chemistry C, 2007. **111**(29): p. 10959-10964.
12. Atourki, L., et al., *Numerical study of thin films CIGS bilayer solar cells using SCAPS.* Materials Today: Proceedings, 2016. **3**(7): p. 2570-2577.
13. Burgelman, M., P. Nollet, and S. Degrave, *Modelling polycrystalline semiconductor solar cells.* Thin solid films, 2000. **361**: p. 527-532.
14. Patel, M. and A. Ray, *Enhancement of output performance of Cu2ZnSnS4 thin film solar cells—A numerical simulation approach and comparison to experiments.* Physica B: Condensed Matter, 2012. **407**(21): p. 4391-4397.
15. Koishiyev, G.T., et al., *Analysis of impact of non-uniformities on thin-film solar cells and modules with 2-D simulations.* 2010.
16. Sreejith, M., et al., *Tuning the properties of sprayed CuZnS films for fabrication of solar cell.* Applied physics letters, 2014. **105**(20): p. 202107.
17. Su, R., et al., *Dielectric screening in perovskite photovoltaics.* Nature communications, 2021. **12**(1): p. 1-11.
18. Gezgin, S.Y., *Modelling and investigation of the electrical properties of CIGS/n-Si heterojunction solar cells.* Optical Materials, 2022. **131**: p. 112738.
19. Yiğit Gezgin, S. and H.Ş. Kiliç, *The effect of Ag plasmonic nanoparticles on the efficiency of CZTS solar cell: an experimental investigation and numerical modelling.* Indian Journal of Physics, 2023. **97**(3): p. 779-796.
20. Adewoyin, A.D., M.A. Olopade, and M. Chendo, *Enhancement of the conversion efficiency of Cu2ZnSnS4 thin film solar cell through the optimization of some device parameters.* Optik, 2017. **133**: p. 122-131.
21. Houimi, A., et al., *Numerical analysis of CZTS/n-Si solar cells using SCAPS-1D. A comparative study between experimental and calculated outputs.* Optical Materials, 2021. **121**: p. 111544.
22. Niane, D., et al., *Generation and Recombination of a CIGSe Solar Cell under the Influence of the Thickness of a Potassium Fluoride (KF) Layer.* American Journal of Materials Science and Engineering, 2018. **6**(2): p. 26-30.
23. Abderrezek, M. and M.E. Djeghlal, *Contribution to improve the performances of Cu2ZnSnS4 thin-film solar cell via a back surface field layer.* Optik, 2019. **181**: p. 220-230.
24. Sun, H., et al., *Efficiency enhancement of kesterite Cu2ZnSnS4 solar cells via solution-processed ultrathin tin oxide intermediate layer at absorber/buffer interface.* ACS Applied Energy Materials, 2017. **1**(1): p. 154-160.
25. Guirdjebaye, N., et al., *Numerical analysis of CdS-CIGS interface configuration on the performances of Cu (In, Ga) Se2 solar cells.* Chinese Journal of Physics, 2020. **67**: p. 230-237.
26. Mounkachi, O., et al., *Band-gap engineering of SnO2.* Solar Energy Materials and Solar Cells, 2016. **148**: p. 34-38.